

Transworld Research Network
37/661 (2), Fort P.O., Trivandrum-695 023, Kerala, India



Beyond Standard Quantum Chemistry : Applications From Gas to Condensed Phases,
2007: ISBN: 978-81-7895-293-2 Editor: Ramón Hernández-Lamonedá

The application of quantum Monte Carlo to the spectroscopy of metallic molecules

A. Ramírez-Solís^{*1} and Michel Caffarel²

¹Dept. of Chemistry and Biochemistry, University of California at Santa Barbara, Santa Barbara, California 93106-9510, U.S.A.

²Laboratoire de Chimie et Physique Quantiques, CNRS-UMR 5626 IRSAMC Université Paul Sabatier, 118 route de Narbonne 31062 Toulouse Cedex, France

Abstract

It is illustrated that quantum Monte Carlo can be a very useful tool for studying key problems in the spectroscopy of metallic molecules. For atomic metallic systems we have recently shown that all-electron fixed-node diffusion quantum Monte Carlo (FN-DMC) leads to results of a quality similar to that obtained with benchmark ab initio calculations [M. Caffarel,

^{*}On sabbatical leave from Depto. De Física, Facultad de Ciencias, Universidad Autónoma del Estado de Morelos, Cuernavaca, Morelos 62209 México

Correspondence/Reprint request: A. Ramírez-Solís, Dept. of Chemistry and Biochemistry, University of California at Santa Barbara, Santa Barbara, California 93106-9510, U.S.A.

*J.P. Daudey, J.L. Heully, and A. Ramírez-Solís, J. Chem. Phys. 123, 094102 (2005)]. In the complex paradigmatic molecular case of CuCl_2 presented here, the spatial distribution of fundamental quantities such as the ground state spin-density (SD) derived from FN-DMC are found to be qualitatively different from those of the standard *ab initio* or DFT methods. From a general perspective, we propose that spin and charge properties obtained for transition metal-containing molecules using accurate FN-DMC calculations should be used as input information in the parametrization of newer and more reliable exchange and correlation functionals.*

I. Introduction

In recent years, quantum Monte Carlo (QMC) has been applied successfully to a number of electronic systems including atoms, molecules, liquids, and solids (e.g[1-9] and references in [10]). The quality of the results obtained is in general impressive, the accuracy achieved is comparable or even superior to that of standard high-quality *ab initio* methods (e.g Coupled Cluster with large basis set). However, the vast majority of the systems studied so far involves only light elements of the first and second rows with small variations of the electronic density. In sharp contrast, very little has been done for the description of complex systems where the electronic density structure is much more intricate. A prototypical example of such complexity is found in transition metal systems. From a general perspective, the physico-chemical and spectroscopic properties of metal-containing molecules are extremely difficult to describe accurately with the available electronic structure methods and this one of the key issues of modern computational quantum chemistry. As well known, this difficulty arise from the electronic complexity involved when many electrons are localized in a small spatial region, for instance, in the 3d and 4d shells of the transition metal family. However, for a wide variety of cases, the understanding of the basic process at work in these metal-containing systems requires quantitatively a high degree of accuracy on the transition energies between the low-lying electronic states.

Up to date very few QMC studies have addressed this most important problem (for references, see [11]). Furthermore, all these studies rely on the use of effective core potentials (ECP) to reproduce the effect of the innermost electrons. It has been shown that the systematic bias associated with the use of ECP in QMC (the so-called “localization” error) can be difficult to control for metallic systems when spectroscopic quantities are searched for [11], [12]. In a recent network [11] we have shown that it is actually possible to perform *all-electron* quantum Monte Carlo calculations for such systems, thus escaping from this difficulty. More precisely, using all-electron Fixed-Node Diffusion Monte Carlo (FN-DMC) calculations we have been able to accurately compute the transition energies between the low-lying electronic states of the copper

atom and its cation, the states being the most relevant ones for the organo-metallic chemistry of copper-containing systems. To the best of our knowledge, this work has provide the most accurate correlation energies ever calculated for these levels. This remarkable result must be considered as a first step towards the applicability of QMC to the study of the physico-chemical properties of transition metal-containing systems.

Here, we go one step further by presenting DMC simulations for a difficult *molecular* case, namely the CuCl_2 molecule.

Before doing that, let us recall briefly the basic ideas of quantum Monte Carlo in its two most popular versions, namely the Variational Monte Carlo (VMC) and Fixed-Node Diffusion Monte Carlo (FN-DMC) approaches. QMC methods being relatively new and, by far, of a much more confidential use than standard *ab initio* wavefunction-based and DFT methods, we think that such a presentation can be useful.

II. Quantum Monte Carlo

In a quantum Monte Carlo scheme a series of “states”, or configurations”, or “walkers” are generated using some elementary stochastic rules. Here, a configuration is defined as the set of the $3N$ -electronic coordinates (N number of electrons), the positions of the nuclei being fixed (within the Born-Oppenheimer approximation)

$$\vec{R} = (\vec{r}_1, \dots, \vec{r}_N). \quad (1)$$

Stated differently, a configuration \vec{R} may be viewed as a “snapshot” of the molecule showing the instantaneous positions of each electron. Stochastic rules are chosen so that configurations are generated according to some target probability density, $\Pi(\vec{R})$. Note that the probability density is defined over the complete $3N$ -dimensional configuration space and not over the ordinary 3D space. Many variants of QMC can be found in the literature (referred to with various acronyms: VMC, DMC, PDMC, GFMC, etc...). They essentially differ by the type of stochastic rules used and/or by the specific stationary density produced. In practice, the two most popular QMC approaches used for simulating complex molecular systems are the so-called Variational Monte Carlo (VMC) and fixed-node Diffusion Monte Carlo (FN-DMC) methods.

A. Variational Monte Carlo (VMC)

In a VMC calculation the probability density generated is given by

$$\Pi_{VMC}(\vec{R}) = \psi_T^2(\vec{R}) \quad (2)$$

where ψ_T is a high-quality electronic trial wavefunction. The standard expression used in VMC for ψ_T consists of a product of two terms. The first term is introduced to describe the one-particle shell-structure of molecules. It is obtained from a preliminary HF or DFT *ab initio* calculation and is expressed as one (or a combination of a few) determinant(s) of single-particle orbitals. The second term is more original and is introduced to reproduce the electron-electron cusp condition of the exact wavefunction and, also, to incorporate some explicit coupling between electron-nucleus and electron-electron coordinates. [13]. Note that the electron-electron cusp condition is known to be particularly difficult to fulfill in standard *ab initio* calculations using expansions over one-electron basis sets (due to the $1/l^4$ - behavior of the energy convergence one must consider very high values of the orbital angular momentum l to obtain accurate results). The explicitly correlated term is usually referred to as the Jastrow factor. In the spin-free formalism used in QMC this trial wavefunction is written as

$$\psi_T(\vec{R}) = D^\dagger(\vec{R})D^\downarrow(\vec{R}) \exp \left[\sum_{\alpha} \sum_{\langle i,j \rangle} U(r_{i\alpha}, r_{j\alpha}, r_{ij}) \right] \quad (3)$$

where the sum over α denotes as sum over the nuclei, $\sum_{\langle i,j \rangle}$ a sum over the pair of electrons, and D^σ ($\sigma = \uparrow$ or \downarrow) are determinants made of one-particle space-orbitals. Different expressions for the Jastrow part have been presented in the literature. Here, we shall use the “minimal” standard form written as follows

$$U(r_{i\alpha}, r_{j\alpha}, r_{ij}) = \frac{a_\sigma r_{ij}}{1 + b_\sigma r_{ij}} - c_\alpha (r_{i\alpha} + r_{j\alpha}) \quad (4)$$

where a_σ, b_σ can take two different values depending on the spin of the pairs of electrons considered. In this latter expression the quantities $\{a_\sigma, b_\sigma, c_\alpha\}$ play the role of variational parameters.

The numerical method (stochastic rules) employed to generate the *known* VMC density, Eq. (2), is a standard Monte Carlo approach based on the use of a generalized Metropolis algorithm. In practice, the walkers are moved using a Langevin-type stochastic differential equation

$$\vec{R}_{new} = \vec{R}_{old} + \vec{b}[\vec{R}_{old}]\tau + \sqrt{\tau}\vec{\eta}, \quad (5)$$

where τ is an elementary time-step, \vec{b} is the so-called drift vector given by

$$\vec{b} = \frac{\vec{\nabla}\psi_T}{\psi_T}, \quad (6)$$

and $\vec{\eta}$ is a gaussian vector made of $3N$ independent gaussian numbers with zero mean and unit variance. Each elementary move \vec{R}_{new} is considered as “trial” move and is accepted or rejected according to the acceptance probability $q \in (0, 1)$ given by

$$q \equiv \text{Min}\left[1, \frac{\psi_T^2(\vec{R}_{new})p(\vec{R}_{new} \rightarrow \vec{R}_{old}, \tau)}{\psi_T^2(\vec{R}_{old})p(\vec{R}_{old} \rightarrow \vec{R}_{new}, \tau)}\right], \quad (7)$$

where $p(\vec{R}_{old} \rightarrow \vec{R}_{new}, \tau)$ is the transition probability density corresponding to Eq.(5), namely

$$p(\vec{R}_{old} \rightarrow \vec{R}_{new}, \tau) = \frac{1}{(2\pi)^{3N/2}} \exp\left\{-\frac{1}{2\tau}[(\vec{R}_{new} - \vec{R}_{old} - \vec{b}_{old}\tau)^2]\right\}. \quad (8)$$

When the move is rejected the new position of the walker is considered to be the old one. It can be easily shown that this generalized Metropolis algorithm admits ψ_T^2 , Eq.(2), as stationary density (see, e.g [14]).

Now, to calculate the variational energy associated with the trial wavefunction

$$E_0^{VMC} = \frac{\langle \psi_T | H | \psi_T \rangle}{\langle \psi_T | \psi_T \rangle} \geq E_0^{exact} \quad (9)$$

we just need to average the so-called local energy at each Monte Carlo step

$$E_0^{VMC} = \lim_{P \rightarrow +\infty} \frac{1}{P} \sum_{i=1}^P E_L[\vec{R}^{(i)}], \quad (10)$$

where the local energy is defined as

$$E_L(\vec{R}) \equiv H\Psi_T/\Psi_T, \quad (11)$$

and the superscript (i) labels the successive configurations. Note that for a *finite* number of Monte Carlo steps P , the variational energy is obtained with a finite statistical error δE which goes to zero as $1/\sqrt{P}$.

A critical step in the VMC approach is the optimization of the parameters entering the trial wavefunction. A standard method consists in searching for parameters minimizing the fluctuations in configuration space of the local

energy. This criterion is based on the fact that for the exact wavefunction the local energy reduces everywhere to a constant -the exact energy- and, thus, the fluctuations of the local energy entirely vanish. Accordingly, small fluctuations are associated with “good” trial wavefunctions. A number of methods have been developed to perform efficiently the optimization step within a QMC framework. Probably the most common one is the correlated sampling method of Umrigar *et al.* [15], an approach based on the minimization of the weighted variance of the local energy over a set of fixed configurations. Note that, very recently, efficient methods based on the direct minimization of the total energy have also been proposed (see, Refs.[16],[17]).

Once the optimal parameters have been determined, the quality of the resulting trial wavefunction is usually good. When using sophisticated Jastrow part [generalizations of Eq.(4), see *eg* Ref.[13]] a major part of the dynamical correlation energy (Coulomb hole) is recovered and the *gross* features of the one-particle back ground are also correctly described via the determinantal part (no-dynamical correlation). For most atoms it is possible to recover up to 80% – 90% of the exact correlation energy [13]; for molecules, the domain of variation lies usually between 30 and 90%.

B. Fixed-node diffusion Monte Carlo(FN-DMC)

In a diffusion Monte Carlo scheme the stochastic rules employed are the same as in the VMC case previously described (generalized Metropolis algorithm based on a Langevin move) plus a new rule corresponding to a branching (or birth-death) process. More precisely, depending on the magnitude of the local energy a given walker can be destroyed (when the local energy is greater than some estimate of the exact energy) or duplicated a certain number of times (local energy lower than the estimate of the exact energy). In practice, the branching step is very easy to implement. After each move the walker is copied a number of times equal to

$$M = \text{Int}[\exp \{-(E_L - E_T)\tau\} + u] \quad (12)$$

where $\text{Int}[]$ is the integer part of a real number, E_T some reference energy, and u an uniform random number defined over $(0,1)$. This expression is built so that *in average* the number of copies is equal to the branching weight $\exp \{-(E_L - E_T)\tau\}$. Remark that the total number of walkers can now fluctuate and, thus, some sort of population control is required. Indeed, nothing prevents the total walker population from exploding or collapsing entirely. Various solutions to this problem have been proposed. The most popular approaches consists either in performing from time to time a random deletion/duplication step or in varying slowly enough the reference energy, E_T , to keep the average number of walkers approximately constant.

It can be shown that the stationary density resulting from these rules is given by

$$\Pi_{DMC}(\vec{R}) = \psi_T(\vec{R})\phi_0(\vec{R}) \quad (13)$$

where $\phi_0(\vec{R})$ denotes the unknown ground-state wavefunction. It is easy to verify that the exact energy is, in the same way as in VMC, obtained as the average of the local energy over the DMC density:

$$E_0^{DMC} = \lim_{P \rightarrow +\infty} \frac{1}{P} \sum_{i=1}^P E_L[\vec{R}^{(i)}]. \quad (14)$$

Actually, because the density Π_{DMC} is necessarily positive (as any stationary density resulting from some stochastic rules), ϕ_0 is not precisely the exact ground-state wavefunction but some approximate one, still solution of the Schrödinger equation but with additional constraint that ϕ_0 has the same sign as the trial wavefunction (so that the product in Eq. (13) remains always positive). Such a constraint implies that the nodes of ϕ_0 (values of \vec{R} for which the wavefunction vanishes) are identical to those of the approximate wavefunction ψ_T . The resulting error is called the “fixed-node” error. Generally, this approximation is very good, the fixed-node error on total energies representing a few percents of the total correlation energy. Finally, it can be shown that the fixed-node energy is an upper bound of the exact energy (so that FN-DMC is a truly variational method)

$$E_0^{FN-DMC} \geq E_0^{exact}. \quad (15)$$

The interested reader can find more details about the various QMC algorithms in several excellent reviews, *e. g.* [10],[18]. For the more specific details of the implementation of FN-DMC to transition-metal systems, the reader is referred to our recent work on the spectroscopy of the copper atom. [11].

III. *Ab initio* and DFT results for the spectroscopy of CuCl_2

The spectroscopy of the CuCl_2 molecule is a particularly difficult case for *ab initio* and DFT methods, since correlation effects arising mainly in the 3d shell of copper are very important; fortunately, the low-lying transitions are experimentally quite well known [19],[20]. The accurate determination of such effects by *ab initio* techniques imperatively requires large optimized basis sets and extensive treatment of correlation effects through multireference CI

(MRCI), coupled cluster singles-doubles and perturbative triples [CCSD(T)], or coupled pair functional (CPF)-derived methods [21], generally using orbitals obtained through rather sophisticated CASSCF algorithms if one aims at providing accurate enough energies to compare with experimental data[22]. On the other hand, since the lowest five electronic states (all doublets) of $CuCl_2$ belong to different spatial symmetries, it has been possible to study these states through the Δ SCF approach in the DFT framework [22],[23],[24]. In this approximation each state, which is the ground state for a given spin and space symmetry, is optimized independently. Therefore, the main goal of [25] was to perform a coherent assessment of DFT results with benchmark *ab initio* calculations, eliminating the discrepancies found in previous studies so that the comparison was restricted to the basic ideas of DFT. The DFT calculations were done with the same RECP and optimized extended basis sets used in Refs. [22] and [26]. In order to understand the extraordinary complexity in the spectroscopic description involving the five lowest ligand-field (LF) and charge-transfer (CT) states note that, at the doubly ionic limit, $CuCl_2$ is described by the $CTCu^{2+}(3d^9)CT$ structure, while in the covalent $ClCuCl$ description, the copper atom which is promoted to the $3d^94s^2$ excited state undergoes 4s-4p hybridization and can establish covalent bonds with both Cl atoms. An intermediate situation arise when one considers the resonant $CTCu^+(3d^94s^1)Cl$ and $ClCu^+(3d^94s^1)CT$ ionic structures. Near the equilibrium distance, the exact electronic structure for all states in a mixture of these three valence situations. The first three LF states ($^2\Sigma_g^+$, $^2\Pi_g$, $^2\Delta_g$) correspond to d-d transitions on the copper ion and they can be described by the σ , π or δ orientations of the singly occupied 3d orbital. It is now known that a correct description of electronic structures, and even more with such close lying states, must include a correct description of correlation effects especially important for the d shell, but also must allow for larger polarization differential effects between localized d-d states and charge transfer states. We stress that single-reference methods like the CPF and CCSD(T) ones can be used, since the HF wavefunctions are excellent zeroth-order approximations for all states of $CuCl_2$ [21]. From the DFT perspective, this feature is also a very good point, since standard DFT-based methods should, in principle, be well adapted to describe transitions where only a change in the orientation of the 3d-hole in the central metal atom is involved. The $^2\Pi_g \rightarrow ^2\Sigma_g^+$ transition represents a most difficult problem from the quantum theoretical point of views in since it has been predicted to range from -2495 to 5887 cm^{-1} . Table I presents some selected DFT-derived (LDA, GGA, hybrid and meta) and the *ab initio* $^2\Pi_g \rightarrow ^2\Sigma_g^+$ transition energies.

Note that, within the *ab initio* framework, the dynamic correlation effects that control the nature of the Cu 3d-hole in the ground state are extremely difficult to obtain correctly since the SCF, the SDCI, and even the usually very

Table I. DFT (vertical) transition energies in wavenumbers compared with *ab initio* and experimental results.

Method	$X^2\Pi_g - ^2\Sigma_g^+$	Ordering ^c /HF exch. in %
LDA(S+VWN5)	6539	w
mPW1K	-1161	w/42.7%
BLYP	4802	w
PBE96	4699	w
HCTH407	4345	w
TPSS	4065	w/1.00 ^d
OPTX-LYP	3963	w/1.43 ^d
B3LYP	1703	c/20%
B97-2	1465	c/21%
PBE0	756	c/25%
NR-LSDA	5574	
NR-GGA	5900	
VWN-BP	4758	
NR-SCF	- 2495	
CASSCF(21,14)	6930	
CASPT2	3861	
NR-SDCI	- 2116	
NR-SDCI+Q	- 1856	
CCSD(T)	859	
NR-CPF	659	
CASSCF(21,14)+ ACPF	232	
Theor. ^a	900	
Expt. ^b	253,303,475	

^a Theoretical SO deconvoluted value from [22].

^b Experimental fine-structure transition energies; see corresponding cited theoretical references in [25].

^c c or w stand for correct or wrong state ordering; %HF exchange quoted where applicable.

^d Care must be taken since for these functionals the sum of the non-local exchange differs from the standard definition.

accurate but non-variational SDCI+Q (with Davidson's correction) schemes, all wrongly lead to a $^2\Sigma_g^+$ ground state. Only much more sophisticated size-consistent *ab initio* methods like the CPF, CCSD(T) or CASSCF+ACPF ones are able to produce a $^2\Pi_g$ ground state, lying only 659,859 and 232 cm^{-1} (respectively) below the $^2\Sigma_g^+$ one, without spin-orbit effects; these transition energies must be compared with the theoretical SO-deperturbed value, estimated to be 900 cm^{-1} [22]. The most challenging question, and its this one we shall be focusing on from here onwards, concerns the way the different DFT approximations (local, semi-local, no-local hybrid and non-local meta-) treat the exchange and correlation effects that, in a very subtle manner, control whether the ground state is of $^2\Pi_g$ or $^2\Sigma_g^+$ nature. Note that most functionals

(GGA, hybrid and even meta-ones) like HCTH407, BLYP, PBE96, OptX-LYP and TPSS largely overestimate this transition, all yielding values above 4000 cm^{-1} . It is really surprising to find out that two semi-empirical hybrid functionals (PBE0 and B97-2) can provide such accurate transition energies, when even very large CASSCF+CASPT2 calculations perform as badly as most of the other functionals for the LF excitations. From examination of table I it appears clearly that the PBE0 hybrid functional provides a result (around 750 cm^{-1}) in excellent agreement with the benchmark *ab initio* CASSCF+ACPF SO-deperturbed value of 900 cm^{-1} [22]. The B3LYP functional *exaggerates* this energy by more than 100%, placing it around 1700 cm^{-1} . The B97-2 functional performs even better than the very popular B3LYP for this case. In order to connect this with the QMC calculations to follow, it is crucial to note here that scalar relativistic (Darwin and mass-velocity) effects cancel out for the energy differences and are negligible on this transition, as shown by the very similar non-relativistic-CPF, and relativistic CCSD(T) and ACPF results. Therefore, the main source of error comes from the differential correlation energy associated with the σ or π orientation of the 3d hole on the central metal atom. This is an essential point since it allows us to make *non-relativistic* all-electron FN-DMC simulations to describe this transition on CuCl_2 . It is important to stress that, given the complexity of this problem, only three semi-empirical hybrid functionals provide accurate transition energies and, therefore, the role of the non-local HF exchange seems to be crucial to compensate the errors made on the correlation contributions to correctly describe the transition energy between these two states. This compensation of errors has recently been shown to occur for the same transition in the AgCl_2 molecule [27], where the optimal weight of the exact HF exchange was found to be 42%, instead of the usual 20% in the B3LYP hybridization of the exchange energy; however, this larger weight makes both equilibrium geometries get considerably longer than the benchmark CASSCF+ACPF ones. Note that up to date, it is impossible to decide *a priori* which functional is to be used and which can be trusted to yield reliable transition energies. The delicate issue of the parametrization of all the existing xc functionals without the inclusion of transition metal containing systems has been discussed extensively [25] in this context. It is somewhat ironic that much less expensive and sophisticated descriptions such as those given by the PBE0 (750 cm^{-1}) and the B97-2 (1400 cm^{-1}) functionals yield better approximations to this transition energy than the very computational demanding benchmark CASSCF+ACPF one at 232 cm^{-1} . So the natural question arises: are these hybrid PBE0 and B97-2 densities really accurate for each electronic state, therefore providing truly accurate total energies, or is this energy difference hiding some cancellation of errors associated with physically relevant quantities, such as the spatial distribution of charge and spin densities?

IV. Charge and spin densities: DFT *vs.* *ab initio* descriptions

In order to answer this question we show in table II the values of several LDA, GGA and hybrid DFT-derived Mulliken charges and spin-densities on the central Cu atom against the very accurate *ab initio* CASSCF figures. The equilibrium geometries of the five lowest-lying electronic states are also shown to stress the fact that, inspite that the transition energies obtained with the hybrid PBE0 and B97-2 empirical functionals are in good agreement with the benchmark *ab initio* ones, the shape and the relative position of the minima for the two-lowest lying is reversed, with a DFT ${}^2\Sigma_g^+$ state around 0.06 bohr longer than the ${}^2\Pi_g$ one, while the CASSCF and ACPF descriptions predict exactly the opposite. A rather different picture of the charge and spin-density distribution is obtained with the DFT-derived methods *vs.* the corresponding *ab initio* ones, especially for the ${}^2\Pi_g$ state. Interesting remarks arise from the comparison of the CASSCF (21, 14) and DFT Mulliken charges on Cu. At the CASSCF level, all the LF states are rather ionic, the ${}^2\Pi_g$ ground state presents a Cu Mulliken net charge of +0.63, while the ${}^2\Delta_g$ state shows a net charge of +0.69. The DFT-based Mulliken charges on Cu differ significantly from one functional to the other. For instance, while the best performing-functional (PBE0) leads to Cu Mulliken charges of 0.18, 0.34 and 0.20 for the ${}^2\Pi_g$, ${}^2\Sigma_g^+$ and ${}^2\Delta_g$ LF states respectively, for the CT states these charges are almost identical, 0.18 (${}^2\Pi_u$) and 0.16 (${}^2\Sigma_u^+$) to that of the ground state; these are actually quite counterintuitive and unexpected results, since the large difference in ionicity between the CT and LF states has usually been highlighted. The last remark concerning the Mulliken charges is that the bad-performing functionals produce almost covalent and ${}^2\Delta_g$ LF states, while the ${}^2\Sigma_g^+$ state appears with a slightly larger cu charge of around 0.22. A particularly rich discussion arises upon analysis of the spin density (SD) results for several of the functionals used. It is quite remarkable that the quality of the excitation spectrum obtained with these functionals can, qualitatively, be related to the magnitude of the spin-density on the central metal atom, since although all the functionals yield SD (Cu) values close to 1.05 for the ${}^2\Sigma_g^+$ and ${}^2\Delta_g$ LF states, the corresponding value for the $X^2\Pi_g$ ground state shows variations one order of magnitude larger (around 0.14) between the good and bad-performing functionals; the PBE0 SD (Cu) value is 0.64 while the BLYP and PBE96 spin-densities on copper are only 0.43. An intermediate situation arises for the next two best performing functionals, B3LYP and B97-2, with larger values of 0.54 and 0.57. As expected, the SD (Cu) values for the CT states is close to zero for all the functionals, since the open shell for these *ungerade* states resides mainly on both Cl atoms. The benchmark CASSCF (21,14) Mulliken spin-densities are

Table II. Comparison of the DFT-derived Mulliken charges (Q) and spin-densities (SD) on Cu vs. the benchmark CASSCF *ab initio* values for selected functionals. Equilibrium Cu-Cl geometries for the symmetric stretching mode of CuCl_2 (bohr) in the five lowest electronic states.

Functional	$X^2\Pi_g$	$^2\Sigma_g^+$	$^2\Delta_g$	$^2\Pi_u$	$^2\Sigma_u^+$
PBE96:					
Re	3.93	3.97	4.00	4.12	4.12
Q(Cu), SD(Cu)	0.02, 0.43	0.24, 1.03	0.02, 1.05	0.04, -0.01	0.04, -0.04
BLYP:					
Re	3.96	4.01	4.03	4.16	4.17
Q(Cu), SD(Cu)	0.04, 0.43	0.22, 1.04	-0.02, 1.05	-0.02, 0.0	-0.03, -0.03
B3LYP:					
Re	3.93	3.98	4.00	4.15	4.17
Q(Cu), SD(Cu)	0.16, 0.57	0.32, 1.07	0.16, 1.04	0.18, -0.02	0.16, -0.07
B97-2:					
Re	3.92	3.96	3.98	4.13	4.14
Q(Cu), SD(Cu)	0.20, 0.54	0.36, 1.03	0.18, 1.03	0.12, 0.0	0.06, -0.10
PBE0:					
Re	3.90	3.96	3.98	4.12	4.13
Q(Cu), SD(Cu)	0.18, 0.64	0.34, 1.08	0.20, 1.05	0.18, -0.01	0.16, -0.09
CASSCF(21,14):					
Re	3.98	3.89	4.01	4.15	4.16
Q(Cu), SD(Cu)	0.63, 0.94	0.66, 1.00	0.69, 1.00	0.38	0.46
CPF:					
Re	3.90	3.95	3.98	4.14	4.14
ACPF:					
Re	3.97	3.93	3.99	4.15	4.15
Exp.					
Re	3.85				

available to compare these DFT-derived quantities. The SD values for the three LF states are very close to 1, which suggest that the states actually present a much more localized hole on the central copper atom than any of the DFT calculations provide.

V. Diffusion quantum Monte Carlo calculations for CuCl_2

Given these facts it is clear that another approach, which is basis set-free and excitation degree-free in the electronic correlation treatment is needed to

yield a more reliable $X^2\Pi_g - ^2\Sigma_g^+$ transition energy and which could, at the same time, provide new information to be used as reference concerning the spatial distribution of charge and spin densities along the molecular axis, which appear to vary greatly depending on the *ab initio* or semi-empirical DFT method used. Here, we have used quantum Monte Carlo (QMC), a powerful stochastic method well adapted to this kind of problem. It is our belief that QMC can provide a very interesting alternate way to better understand the complex dynamic correlation effects responsible for the $X^2\Pi_g - ^2\Sigma_g^+$ gap. At the root of a FN-DMC calculation is the choice of the trial wavefunction. The better this wavefunction is, the smallest the statistical and fixed-node errors are. Here, the trial wavefunction is built from a SCF solution for both states, since exact wavefunctions have been shown to have a strong mono-configurational character [21],[22]. Large all-electron ANO-type basis sets were used to build both HF trial wavefunctions; in particular, for Cu we have used the all-electron very large ANO basis set of Bauschlicher [28]. To take into account the electron-electron cusp the simple Jastrow factor, Eq. (4), has been employed. Intensive DMC simulations have been performed, the total number of Monte Carlo steps reaching about 2.2×10^9 for each state. The total ground-state energies obtained are -2560.826 (17) and -2560.785(20) for the $^2\Sigma_g^+$ and $^2\Pi_g$ states, respectively. In wavenumbers the corresponding transition energy is -8998 cm^{-1} with an error bar of 5706 cm^{-1} . Remark that with the standard definition employed here for the error bar, the probability that the exact DMC result is within the interval $-8998 \text{ cm}^{-1} \pm 5706 \text{ cm}^{-1}$ is 68%, while the probability is 95% for an interval two times larger. Clearly, the statistical error is still too large and our result is statistically compatible with almost all results of Table I. To get a more accurate valuation of the transition energy would be very desirable, but in practice it is particularly expensive due to the $1/\sqrt{P}$ -statistical convergence of Monte Carlo simulations (P = number of Monte Carlo steps). Now, although the convergence of energy calculations with the required accuracy to deal with the transition energy appears to be out of reach (recall that the total uncertainty on the difference of energies is the squared root of the sum of the squared uncertainties on the energy of each state), there is a lot of precious information to be extracted from other properties. As mentioned above, particularly interesting quantities are the spin densities. The quantity considered here is the difference of spin densities integrated within the plane perpendicular to the molecular axis (actually, a parallelepiped of small thickness). Our working definition is

$$\Delta\rho(z) = \int_z^{z+\epsilon} dz \int dx dy [\rho_\alpha(\vec{r}) - \rho_\beta(\vec{r})],$$

where z is the coordinate along the molecular axis of the linear molecule, the Copper atom being at the origin, and ϵ is a small positive parameter (here, chosen equal to 0.1 a.u) corresponding to the thickness of the parallelepiped. The α - and β - spin densities have been computed using the distribution of electrons generated during the stochastic simulation [29]. The FN-DMC results are presented in Figs. 1 and 2 for the two lowest states and compared to the results obtained at different levels of theory.

Several important remarks appear upon analysis of the differences observed for the $\Delta\rho(z)$ function obtained for the SCF, CASSCF, and the various DFT approximations. First of all, for both states, the CASSCF (21, 14) curves present very small differences with respect to the SCF ones (for clarity the CASSCF data have thus been omitted in the figures). This is consistent with the fact the HF-SCF wavefunction is an excellent reference for the CPF and CCSD (T) calculations for both, the $X^2\Pi_g$ and $^2\Sigma_g^+$ states, as mentioned before. However, it is remarkable that the FN-DMC spin densities for both states show much larger oscillations with significant change of signs, not only on the outer parts, but also in the bonding regions between the Cu and Cl nuclei. For the $^2\Sigma_g^+$ state note, for example, that while neither the *ab initio* SCF/CASSCF nor any of the increasingly sophisticated local (LDA), semi-local GGA(BLYP) or even the non-local hybrid (PBE0, B3LYP) DFT descriptions provide negative values for the spin-density in the bonding regions,

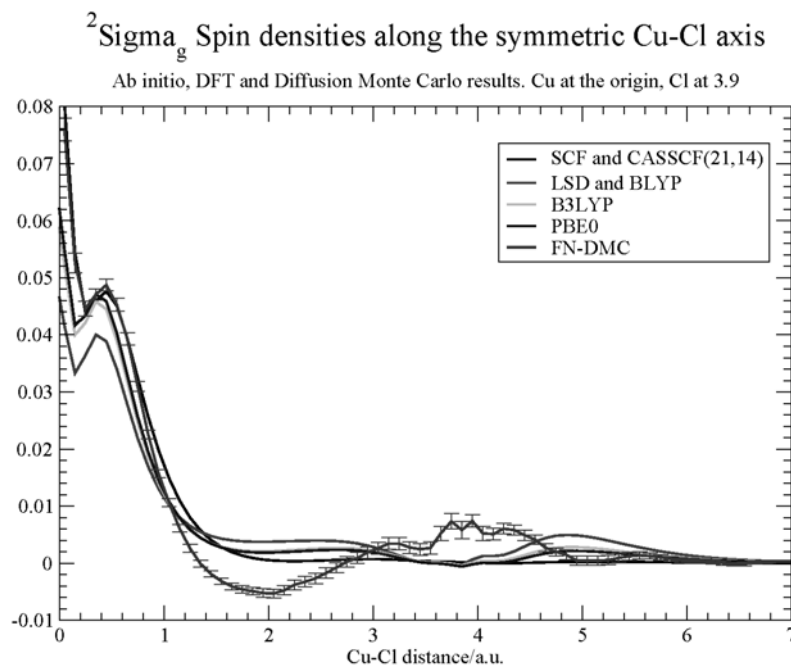


Figure 1. $^2\Sigma_g^+$ state. Integrated difference in spin densities along the molecular axis at different levels of theory. Copper at the origin and both chlorine atoms placed 3.9 bohr on each side.

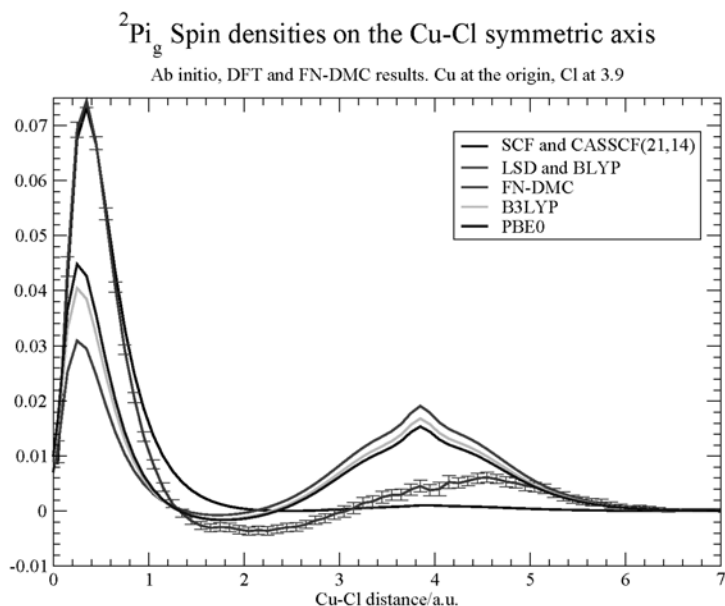


Figure 2. $^2\Pi_g$ state. Integrate difference in spin densities along the molecular axis at different levels of theory. Copper at the origin and both chlorine atoms placed 3.9 bohr on each side.

the FN-DMC spin-density has its most negative value at the midpoint of the Cu-Cl bonds. It is also noteworthy that, while the *ab initio* and the DFT spin-density at the Cl nuclei is nearly zero, the FN-DMC value has there the second largest positive value and shows large oscillations, which actually have the opposite sign of the PBE0 and B3LYP values in the outer regions (beyond 4 bohrs). For the $X^2\Pi_g$ state the discrepancy of the *ab initio* and DFT with FN-DMC results is, qualitatively, even worse, but in different spatial regions for the DFT and for the *ab initio* approaches. Note that while the spin density on the copper atom of every DFT-based method is much smaller than that calculated with *ab initio* SCF or CASSCF methods, the latter provides very good values as compared with FN-DMC ones. On the contrary, in the regions around the Cl nuclei all DFT schemes provide large maxima, while the *ab initio* spin-densities are nearly zero around the halogens; the FN-DMC simulations also provide maxima whose shape resembles the DFT ones, but the absolute values of the spin-densities of these two approaches are shifted along the internuclear axis, so that while the FN-DMC value at the Cl nuclei is very nearly zero, the DFT values are positive and much larger. Once again, in the bonding region large oscillations appear with the FN-DMC spin density which are completely absent with the *ab initio* or any DFT-based method. Overall, it can be concluded that the actual spatial distribution of the spin density for these low-lying states shows a much richer structure, having many more nodes along the molecular axis, than could be anticipated using standard DFT, or for

that matter, even with sophisticated CASSCF *ab initio* approaches. We think these accurate and detailed spin-density curves are conceptually very important and provide lots of relevant information that should be used as basic input for the design of more advanced “non-empirical”, or even to develop more reliable “semi-empirical” hybrid exchange-correlation functionals within the DFT framework. We are currently investigating this important issue; some progress along this path will be presented in a forthcoming publication [30].

VI. Conclusions

We have shown that, in spite of the fact some of the hybrid-type functionals produce very good transition energies between the two lowest-lying electronic states of the paradigmatic CuCl_2 molecule, the spin densities obtained through functionals belonging to all rungs in DFT Jacob's ladder are extremely delocalized along the nuclear axis, when compared to the *ab initio* CASSCF ones. A quite intriguing finding has been obtained concerning the relative quality of benchmark-type *ab initio* spin-densities for the ground and first excited states since, although in a different qualitative manner, these also differ significantly from the FN-DMC ones, particularly near the metal-ligand bonding regions, where even large *ab initio* CASSCF calculations fail at describing the spin-density oscillations and the non-negligible spin-densities in the outer region, found to exist with the FN-DMC approach. This is a particularly relevant since, up to date, no better way than the CASSCF+ACPF method is available to accurately address the electronic structure of transition metal molecules; therefore, we leave this matter as an open question that certainly deserves further investigations. Our conclusion is that the very accurate transition energies obtained by DFT approaches (from high-level approximations in Jacob's Ladder) actually arise from cancellation of errors made in the spatial distribution of spin-densities for the states under study. Now, we hope that the DFT community will take advantage of the present results to improve the way the exchange and correlation functionals are modelled. Certainly, for such complex metallic systems this not an easy task, given the minute energy differences involved in the change of shape of the electronic hole along the molecular axis. Finally, we stress that much physical insight can be gained by analyzing the FN-DMC densities by comparing these with the *ab initio* and DFT-derived ones, and it is expected that clearer view on these very complex electronic systems will emerge from these comparisons.

Acknowledgments

We wish to thank the UAEM supercomputing center (from SEP FOMES-2000 project “Cómputo cientifiCo”), IDRIS (CNRS, Orsay), and CALMIP (Universite Paul Sabtier de Toulouse) for providing us with generous

allocations of superscalar time. ARS thanks CONACYT (México) through Project No.45986 and CMEXUS/CONACYT for sabbatical support at UCSB.

Reference

1. M. Casula, C. Attaccalite, S. Sorela, J. Chem. Phys. **121** 7110 (2004).
2. F. Schautz, F. Buda, C. Filippi J. Chem. Phys. **121** 5836 (2004).
3. A. Aspuru-Guzik, O. El Akramine, J. C. Grossman, and W. A. Lester Jr., J. Chem. Phys. **120** 3049 (2004).
4. A.J. Williamson, J.C. Grossman, R.Q. Hood, A. Puzder, and G. Galli, Phys. Rev. Lett. **89**, 196803 (2002).
5. A. Puzder, A.J Williamson, J.C. Grossman, and G. Galli, J. Chem. Phys. **117**, 6721 (2002).
6. A. Puzder, A.J Williamson, J.C. Grossman, and G. Galli, Phys. Rev. Lett. **88**, 097401(2002).
7. G. Belomoin, E. Rogozhina, J. Therrien, P.V. Braun, L. Abuhassan, M.H Nayfeh, L.Wagner, and L. Mitáš, Phys. Rev. B **65**, 193406 (2002).
8. C. Filippi, S.B. Healy, P. Kratzer, E. Pehlke, and M. Scheffler, Phys. Rev. Lett. **89**, 166102 (2002).
9. A.J. Williamson, R.Q. Hood, and J.C. Grossman, Phys. Rev. Lett. **87**, 246406 (2001).
10. W.M.C. Foulkes, L. Mitáš, R.J. Needs, and G. Rajogopal, Rev. Mod. Phys. **73**, 33 (2001).
11. M. Caffarel, J.P. Daudey, J.L. Heully, and A. Ramírez-Solís, J. Chem. Phys. **123**, 094102 (2005).
12. H.J. Flad and M. Dolg, J. Chem. Phys. **107**, 7951(1997).
13. K.E. Schmidt and J.W. Moskowitz, J. Chem. Phys. **93**, 4172(1990).
14. M. Caffarel, *Introduction to numerical simulations* (in french), ww.lpthe.jussieu.fr/DEA/
15. C.J. Umrigar and K.G. Wilson and J.W. Wilkins, Phys. Rev. Lett. **60**, 1709 (1998).
16. Xi Lin, Hongkai Zhang, and Andrew M. Rappe, J. Chem. Phys. **112**, 2650 (2000).
17. C.J. Umrigar and C. Filippi, Phys. Rev. Lett. **94**, 150201 (2005).
18. B.L. Hammond, W.A. Lester,Jr., and P.J. Reynolds in *Monte Carlo Methods in Ab Initio Quantum Chemistry*, World Scientific Lecture and course notes in chemistry Vol.1 (1994).
19. A.J. Ross, P. Crozet, R. Bacis, S. Churassy, B. Erba, S.H. Ashworth, N.M. Lakin, M.R. Wickham, I.R. Beattie and J.M. Brown, J. Mol. Spectrosc. **177**, 134 (1996); A.J. Bouvier, E. Bosch and A. Bouvier, Chem. Phys. **202**, 139 (1996); E. Bosch, P. Crozet, A.J. Roos and J.M. Brown, J. Mol. Spectrosc. **202**, 253 (2000) and references therein.
20. M. Lorenz, N. Caspary, W. Foeller, J. Agreiter, A.M. Smith and V.E. Bondibey, Mol. Phys. **91**, 483 (1997); M. Lorenz, A.M. Smith and V.E. Bondibey, J. Chem. Phys. **115**, 8251(2002).
21. C.W. Bauschlicher and B.O. Roos, J. Chem. Phys. **91**, 4785 (1989).
22. A. Ramírez-Solís and J.P. Daudey, J. Chem. Phys. **120**, 3221(2004).
23. F. Rogemond, H. Chermette and D.R. Salahub, Chem. Phys. Lett. **219**, 228 (1994).
24. R.J. Deeth, J. Chem. Soc. Dalton Trans. 1061 (1993).

-
25. A. Ramírez-Solís, R. Poteau, A. Vela and J.P. Daudey, *J. Chem. Phys.* 122, 164306 (2005).
 26. A. Ramírez-Solís and J.P. Daudey, *J. Chem. Phys.* 12, 14315 (2005).
 27. A. Ramírez-Solís, R. Poteau and J.P. Daudey, *J. Chem. Phys.* 124, 034307 (2006).
 28. C.W. Bauschlicher, Jr., *Theor. Chim. Acta* 92, 183 (1995). (s,p,d) exponents from H. Partidge, *J. Chem. Phys.* 90, 1043 (1989).
 29. Note that the DMC distribution is given by $\psi_T\phi_0$ when ψ_T is the trial wavefunction and ϕ_0 the exact solution, and not by ϕ_0^2 . Accordingly, there exist a systematic bias when properties other than energy are computed. To reduce this error, we have employed the “second-order” formula mixing the diffusion and variational Monte Carlo results for the spin densities (see Ref. [18]). Although this formula is still not exact, we expect our results to be rather accurate.
 30. M.Caffarel and A.Ramírez-Solís, (2006). Preprint.